2012

Self-assembly and biphasic iron-binding characteristics of Mms6, a bacterial protein that promotes the formation of superparamagnetic magnetite nanoparticles of uniform size and shape

Lijun Wang
Iowa State University

Tanya Prozorov
Iowa State University, tprozoro@ameslab.gov

Pierre E. Palo
Iowa State University, ppalo@iastate.edu

Xunpei Liu
Iowa State University

Follow this and additional works at: http://lib.dr.iastate.edu/cbe_pubs

David Vaknin
Iowa State University, vaknin@ameslab.gov

Part of the Biochemical and Biomolecular Engineering Commons, and the Biological and Chemical Physics Commons

See next page for additional authors

The complete bibliographic information for this item can be found at http://lib.dr.iastate.edu/cbe_pubs/157. For information on how to cite this item, please visit http://lib.dr.iastate.edu/howtocite.html.

Authors

Lijun Wang, Tanya Prozorov, Pierre E. Palo, Xunpei Liu, David Vaknin, Ruslan Prozorov, Surya K. Mallapragada, and Marit Nilsen-Hamilton

Self-Assembly and Biphasic Iron-Binding Characteristics of Mms6, A Bacterial Protein That Promotes the Formation of Superparamagnetic Magnetite Nanoparticles of Uniform Size and Shape

Lijun Wang,[†,‡] Tanya Prozorov,[†,§] Pierre E. Palo,[†] Xunpei Liu,[†,§] David Vaknin,[†] Ruslan Prozorov,[†,‖] Surya Mallapragada,[†,§] and Marit Nilsen-Hamilton*[,†,‡]

[†]Ames Laboratory, U.S. Department of Energy, Ames, Iowa 50011, United States

[‡]Department of Biochemistry, Biophysics and Molecular Biology, [§]Department of Biological and Chemical Engineering, and [‖]Department of Physics and Astronomy, Iowa State University, Ames, Iowa 50011, United States

S *Supporting Information*

ABSTRACT: Highly ordered mineralized structures created by living organisms are often hierarchical in structure with fundamental structural elements at nanometer scales. Proteins have been found responsible for forming many of these structures, but the mechanisms by which these biomineralization proteins function are generally poorly understood. To better understand its role in biomineralization, the magnetotactic bacterial protein, Mms6, which promotes the formation in vitro of superparamagnetic magnetite nanoparticles of uniform size and shape, was studied for its structure and function. Mms6 is shown to have two phases of iron binding: one high affinity and stoichiometric and the other low affinity, high capacity, and cooperative with respect to iron. The protein is amphipathic with a hydrophobic N-terminal domain and hydrophilic C-terminal domain. It self-assembles to form a micelle, with most particles consisting of 20−40 monomers, with the hydrophilic C-termini exposed on the outside. Studies of proteins with mutated C-terminal domains show that the C-terminal domain contributes to the stability of this multisubunit particle and binds iron by a mechanism that is sensitive to the arrangement of carboxyl/hydroxyl groups in this domain.
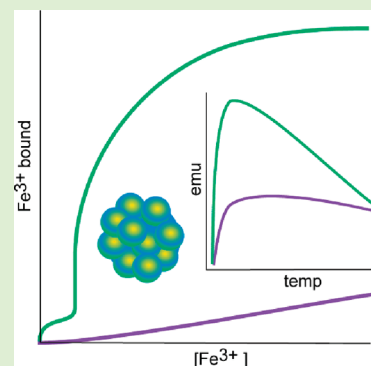
INTRODUCTION

Magnetoreception is a sensory system that provides the orientation, navigation, and homing traits for some creatures from bacteria to higher vertebrates.[1] The physical basis of this response is thought to be the nanoparticles of single-domain magnetite.[2] These nanoparticles have been found in fish, pigeons, honeybees, and even in human brains.[1−3] It is believed that they are responsible for the direction-sensing behaviors of these organisms. The ability to fabricate such fundamental structures independent of these organisms could open many new and exciting opportunities in nanotechnology and materials development.

Magnetotactic bacteria are aquatic prokaryotes that can move under the direction of the local geomagnetic field due to their ability to synthesize magnetite nanoparticles.[4−7] Magnetite nanoparticles of similar size and shape to the bacterial magnetite crystals are formed in vitro in the presence of recombinant Mms6, a magnetosome-associated protein from *Magnetospirillum magneticum* strain AMB-1.[8,9] Although Mms6 alone is not responsible for the formation of magnetite nanocrystals in vivo,[10] its in vitro activity provides us an opportunity for understanding the mechanism(s) by which this biomineralization protein functions.

Here, we demonstrate that Mms6 self-assembles as a micelle with the C-terminal domain on the surface most likely organized as an octamer. The ability of biomineralization proteins to self-assemble into higher order supramolecular structures is believed to be critical in controlling the mineral phase deposition and structure in biomineralization systems such as bone and teeth.[11−14] Although many membrane proteins form mixed micelles with detergents, it is rarely reported that a protein spontaneously self-assembles into a stable micelle in the absence of detergent such as we demonstrate here for Mms6. This characteristic is a feature of the special class of amphiphilic proteins to which Mms6 belongs.[15] Proteins reported to spontaneously form micelles or nanospheres are almost all involved in biomineralization.[16−18] The best studied case is ameloginin, a protein responsible for the formation of enamel, which forms nanospheres that further self-assemble into elongated chain multimers.[19,20] This elongated assembly of ameloginin nanospheres with its large

surface area is believed to be responsible for the formation of enamel.[11]

Our results are consistent with a quaternary structure in which the hydrophobic N-terminal domain of Mms6 anchors the hydrophilic C-terminal domain in the micelle from which the C-terminal domain binds iron and promotes the nucleation and growth of magnetite nanoparticles. The protein exhibits two modes of interaction with iron, one a high affinity stoichiometric interaction and the second a low affinity and high capacity interaction. This latter interaction is proposed as responsible for directing crystal growth. In vivo Mms6 is believed to be a membrane protein, which would enable the C-terminal domain to distribute over the surface of the magnetosome membrane for promoting crystal formation. We propose that its ability to self-assemble in vitro allows Mms6 to form an extended surface of C-terminal domains that can template the crystallization of magnetite.

EXPERIMENTAL SECTION

Materials. The mature form of Mms6 and two mutants (m2Mms6 and m3Mms6) were cloned, expressed, and purified with N-terminal poly histidine tags.[9] The C-terminal sequences of these proteins are Mms6 (KSRDIESAQSDEEVELRDALA), m2Mms6 with −OH and −COOH side chains shuffled (KDRSIDEAQESDSVELREALA) and m3Mms6 with all 21 residues in the C-terminal domain scrambled (QSLERAEDEDADISAVEKLSR). The remaining sequences of these proteins are identical. The 21 amino acid C-terminal region of Mms6, C21Mms6, was synthesized by Genscript Corp. (www.genscript.com).

Analytical Ultracentrifugation. Sedimentation of Mms6 (0.09 mg/mL) in 0.5 mL of 137 mM NaCl, 2.7 mM KCl, 4.3 mM Na_2HPO_4, and 1.4 mM KH_2PO_4, pH 7.2 was monitored at 230 nm in a Beckman analytical ultracentrifuge run at 65520g, 4 °C for 2 h. The sedimentation profile of Mms6 was generated using Ultrascan 8.0.[21−23]

Size Exclusion Chromatography. Chromatography was performed at 4 °C in an AKTA FPLC system (GE healthcare) through prepacked Superose 12 10/300GL and Superdex Peptide 10/300GL columns in the same buffer as for ultracentrifugation. Blue dextran (MM > 2000 kDa) and B12 (MM = 1.3 kDa) were used to determine the void volume and the lower separate limit of the Superose 12 column used. Flow rates were 0.4−0.5 mL/min. All column samples were prepared by centrifugation at 14000g, 4 °C for 1 h before use.

Liposome Preparation. Liposomes consisting of 1-palmitoyl-2-oleoyl-sn-glycero-3-phosphocholine (POPC) and 1,2-dioleoyl-sn-glycero-3-phospho-L-serine (DOPS) were prepared by extrusion through polycarbonate filters.[24]

$^{55}Fe^{3+}$ Binding Assays. Mms6 (100 nM or 1 μM) in 100 mM KCl was incubated with ^{55}Fe (PerkinElmer) as ferric chloride (pH 3) or ferric citrate (pH 7.5) for 2 h at 25 °C. The samples were captured on nitrocellulose filters and washed, and the ^{55}Fe was quantified by liquid scintillation spectrometry.

Dynamic Light Scattering (DLS). Mms6 (0.5 mg/mL) in 100 μL of 137 mM NaCl, 2.7 mM KCl, 4.3 mM Na_2HPO_4, 1.4 mM KH_2PO_4, pH 7.2 at 25 °C was analyzed with a Zetasizer Nanoparticle analyzer (Model: ZEN3690, Malvern Instrument Ltd., Southborough, MA). Each measurement consisted of 11 acquisitions of 10 s with 3 repeats. Data were processed by using Dispersion Technology Software 5.00 (Malvern Instrument Ltd.). The buffer was filtered through a 0.45 μm nitrocellulose membrane and the protein samples were centrifuged for 1 h (14000g, 4 °C) prior to use

Surface Pressure Isotherms. The surface pressure isotherms of Mms6 were measured by a Langmuir−Blodgett trough (Type611, Nima Technology). Mms6 (2.36 μg in buffer) was directly added onto the surface of 500 mL of 20 mM Tris-HCl, 100 mM KCl, pH 7.5 or pH 3 at 25 °C. The surface pressure isotherms were measured at a compression rate of 10 cm^2/min.

Magnetite Nanoparticle Formation. Magnetite nanoparticles were synthesized by coprecipitation of $FeCl_2$ and $FeCl_3$ from aqueous solutions in the presence of Mms6 or its variants as previously reported.[9,25] The proteins to be tested were incubated with iron in Pluronic gel under conditions conducive to the formation of iron oxide crystals. Pluronic F127 polymeric aqueous solutions, which exhibit reverse temperature gelation and form viscous gels at room temperature, were introduced into the synthesis, to slow the diffusion rates of the reagents during particle formation.

Transmission Electron Microscopy Characterization. Magnetite nanoparticles were visualized with a Tecnai G^2 F20 Scanning Transmission Electron Microscope (FEI Company, Hillsboro OR) equipped with high angle annular dark field (HAADF) and energy dispersive X-ray spectroscopy (EDX) detectors at an operating voltage of 200 KV. A 10 μL aliquot of thoroughly washed concentrated suspension of magnetite nanoparticles was dispersed in 3 mL of ddH$_2$O. A 20 μL aliquot of diluted nanoparticle suspension prepared in this manner was deposited on a holey carbon-coated copper grid and dried at room temperature under partial argon flow.

Magnetization Measurements. Magnetization measurements were carried out by using a *Quantum Design* SQUID (Superconducting Quantum Interference Device) 5T MPMS (Magnetic Properties Measurement System). Under moderate argon flow, 30 μL of concentrated, washed nanoparticle suspension was injected into a double-walled polycarbonate capsule. The samples were cooled in a zero applied field to 5K. A negative magnetic field of −5 T was applied to ensure complete remagnetization of all nanocrystals and then reversed to 500 Oe to ensure complete magnetization reversal in each particle and to remove metastable states.

RESULTS

High Affinity Iron Binding by Mms6. The affinity of Mms6 for iron has so far only been demonstrated qualitatively.[8,9] Using ^{55}Fe-citrate as the form of soluble ^{55}Fe, we determined the maximum stoichiometry of iron to Mms6 and the dissociation constant for Mms6 and $^{55}Fe^{3+}$. The stoichiometry was 1 and, taking into consideration the K_d ($10^{−11.5}$ M) of citrate for Fe^{3+}, the K_d of Mms6 for Fe^{3+} was calculated to be $10^{−16}$ M (Figure 1A). Two mutant forms of Mms6 (m2Mms6 and m3Mms6) did not bind Fe^{3+} with high affinity (Figure 1A). To determine the Fe^{3+}-binding ability of the 21 amino acid C-terminal domain of Mms6, C21Mms6, we used size exclusion chromatography because the peptide does not adsorb to the nitrocellulose filters used for the filter assay (Figure 1B). The binding of Fe^{3+} by C21Mms6 was determined to be stoichiometric. Although we did not obtain an affinity constant of the C-terminal domain of Mms6 for Fe^{3+}, the fact that C21Mms6 binds Fe^{3+} stoichiometrically in the presence of excess citrate shows that it has a higher affinity than citrate for Fe^{3+}. These results, along with our previous observation that the C-terminal domain alone can promote the growth of superparamagnetic nanoparticles,[9,25] identify the C-terminal domain of Mms6 as responsible for high affinity stoichiometric iron binding. This conclusion is also supported by the fact that the C-terminal domain (YAYMKSRDIESAQSDEEVELRDALA) is the location of almost all amino acid residues capable of chelating Fe^{2+} or Fe^{3+}, whereas the N-terminal domain (MVGGTIWTGKGLGLGLGLGLGAWGPIILGVVGAGAV) consists of mostly hydrophobic amino acid residues. The polyhistidine tag attached to the N-terminal domain has previously been shown not to promote the formation of superparamagnetic nanoparticles.[9]

Two Distinct Phases of Iron Binding by Mms6. The high affinity constant was determined at pH 7.5 using the Fe^{3+}-citrate equilibrium to establish accurate low levels of free Fe^{3+}. However, nanoparticle formation promoted by Mms6 in vitro is achieved at high iron concentrations that cannot be achieved at
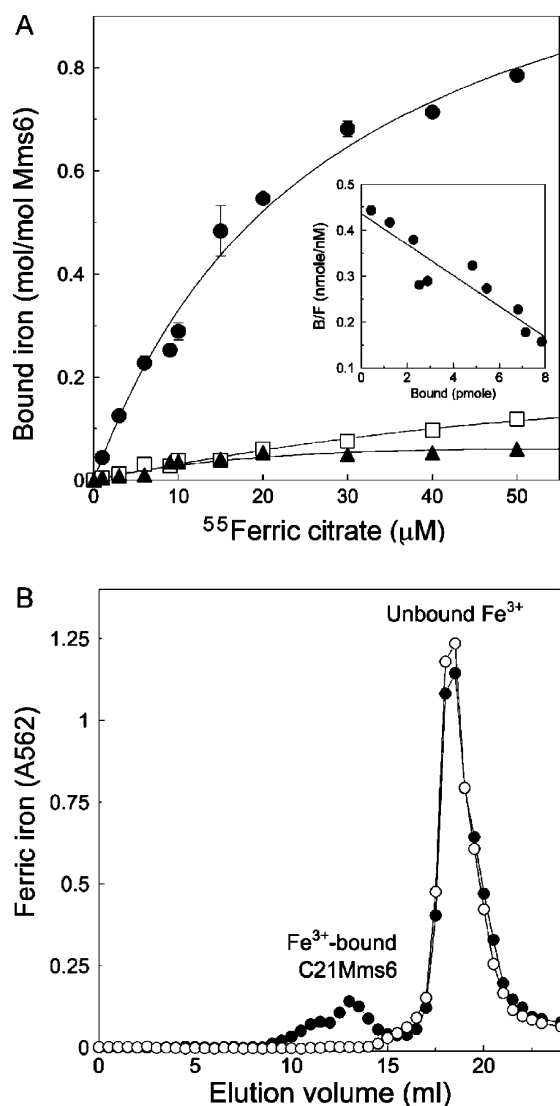
Figure 1. Iron binding characteristics of Mms6. (A) ^{55}Ferric citrate was incubated in duplicate with 1 μM Mms6 for 2 h, followed by capture of the bound iron by the filter assay. Inset: Scatchard plot. Mms6 (●), m2Mms6 (□), m3Mms6 (▲). (B) The elution profile is shown of Fe^{3+}-citrate with (●) or without (○) C21Mms6 from a Superdex peptide 10/300GL column.

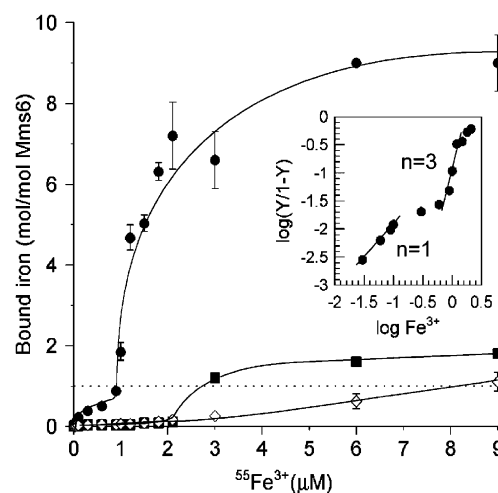**Figure 2.** Two phases of iron binding by Mms6. Binding of Mms6 to free ferric iron was measured using ^{55}FeCl$_3$ with the filter assay. The reaction mixtures contained 100 nM Mms6 (●), m2Mms6 (◇), or m3Mms6 (■) in 20 mM Tris-HCl, 100 mM KCl, pH 3. Incubation was for 2 h at 25 °C followed by collection and analysis by the filter assay. All data are the average of duplicate values. Error bars represent the standard deviations. Inset: Hill plot.

pH 7 due to the insolubility of hydrated Fe^{3+} at neutral pH. Therefore, the concentration dependence of Fe^{3+} binding to Mms6 was also determined at pH 3. Under these conditions, two distinct phases of iron binding by Mms6 were observed (Figure 2). Scatchard plots of the data constituting the first high affinity phase revealed stoichiometric binding (Fe^{3+}/Mms6 = 1:1). A K_d^{app} of 0.58 ± 0.03 μM was measured. A similar value of 0.43 ± 0.11 μM with a stoichiometry of 1.2 ± 0.2 was determined by isothermal titration calorimetry from an average of three experiments at pH 3 (Supporting Information, Figure S3). Thus, the K_d for high affinity binding affinity of iron is significantly lower at pH 3 than pH 7. This result suggests a conformational difference under the two conditions, for which evidence was obtained by CD spectroscopy (Supporting Information, Figure S1).

The second binding phase has a much lower apparent affinity (K_d^{app} = 6 ± 4 μM) with an average of 19 ± 8 (N = 3) irons per Mms6. A Hill plot revealed cooperativity of the second binding

phase of Fe^{3+} binding to Mms6 (Hill n value ~3). The m2Mms6 (shuffled C-terminal −OH and −COOH groups) and m3Mms6 (scrambled C-terminal sequence) were also tested for iron-binding under the same conditions as for Mms6. Both had lower affinities for iron than Mms6 and did not exhibit two phases of iron binding although m3Mms6 displayed low affinity and saturable iron binding (Figure 2). By contrast, the linear increase in binding by m2Mms6 at higher Fe^{3+} concentrations appears to be nonspecific.

Formation of Magnetic Crystals of Uniform Size and Shape Is Associated with a Defined Arrangement of Carboxyl and Hydroxyl Groups in the C-Terminal Domain of Mms6. To determine if the observed iron binding properties of Mms6 might be responsible for its ability to promote the formation of superparamagnetic magnetite crystals of uniform shape and size, Mms6 and the two mutant proteins, m2Mms6 and m3Mms6, were incubated with iron in Pluronic gel under conditions conducive to the formation of iron oxide crystals.[9,25] The particles formed were gathered and examined by transmission electronic microscopy for morphology and size and by the zero field cooled (ZFC-W) procedure to measure magnetic characteristics. The sizes and shapes of the magnetite nanocrystals grown in the presence of Mms6, m2Mms6, m3Mms6, or no-protein were different, with only the Mms6-grown crystals being large, with evidence of a crystalline lattice (Figure 3). Nanoparticles grown with Mms6 showed an elevated blocking temperature (T_B), whereas particles grown in the presence of m2Mms6 showed the same profile as samples that contained no protein (Figure 3). The Mms6-templated magnetite nanocrystals exhibited the behavior closest to that expected of superparamagnetic magnetite particles. These results are consistent with the results of iron binding and suggest that the observed iron-binding properties of Mms6 are responsible for its ability to promote the formation of superparamagnetic crystals.

Mms6 Exists in Aqueous Solution As Micelles. The apparent molecular mass of Mms6 was determined by size exclusion chromatography, analytical ultracentrifugation, and
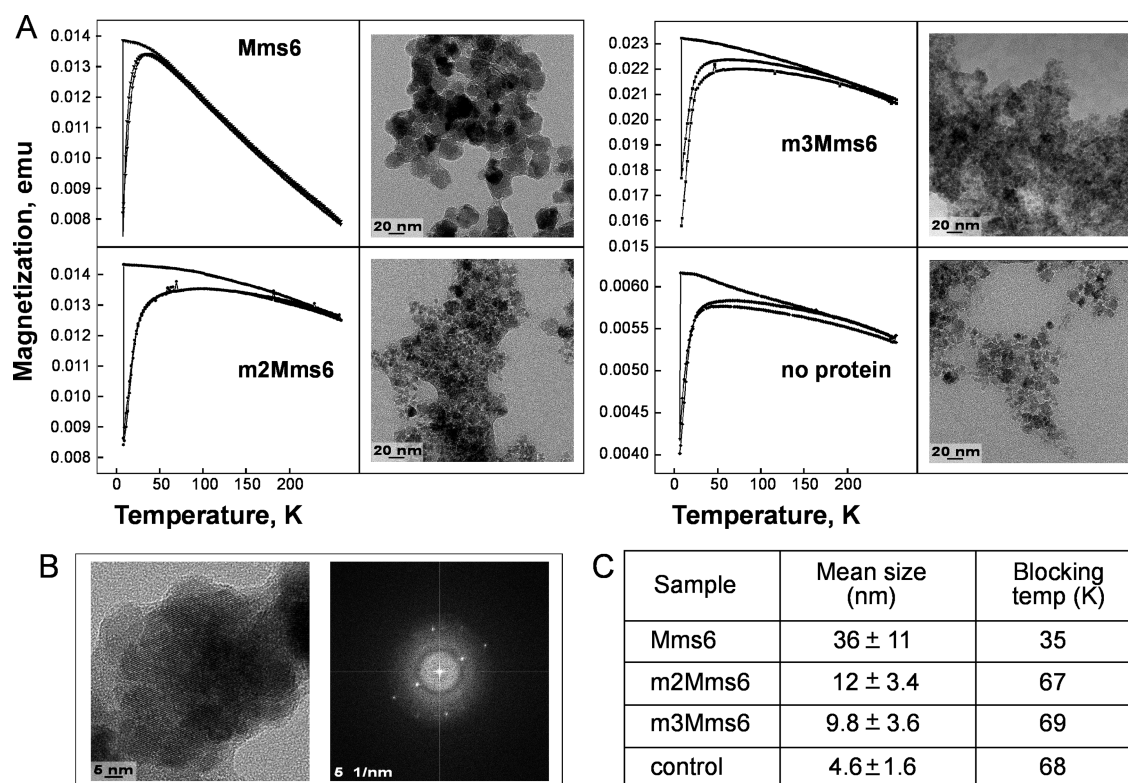
Figure 3. Mms6 promotes the formation of superparamagnetic nanoparticles of uniform size and shape. (A) Temperature-dependencies of magnetization of the magnetite nanocrystals grown in the presence of Mms6, m2Mms6, m3Mms6, or no-protein and TEM images showing their sizes and shapes. (B) Image of magnetite nanocrystals formed in the presence of Mms6 taken at 360000-fold magnification, along with the Fast Fourier Transform that reveals the presence of a crystalline lattice. (C) Mean sizes and blocking temperatures of the particles shown in A. The analysis of magnetite crystal size was performed on numerous micrographs (total > 1000 particles measured) obtained in the bright field mode. Shown are the mean values and the standard deviation of the mean.

DLS (Figure 4A−C). These studies showed that Mms6 exists as large complexes at pH 3 and 7.5. The monomeric molecular mass of Mms6 is 10.2 kDa, but the peak of Mms6 passed through a Superose 12 column with the void volume, which suggests an apparent molecular mass of equal or greater than 300 kDa. Similar results were found at pH 7.5 and 3 in the presence or absence of $FeCl_3$. The observed sedimentation coefficients, distributed from 20 to 100S with the majority between 20 and 40S, also indicate that Mms6 forms large multimers with an estimated apparent molecular mass between 200 and 400 kDa. DLS measurement of Mms6 showed two particle sizes between which the protein mass is almost equally distributed. Peak 1 was 59% of the mass containing particles of 5.1 ± 1.5 nm radius with an estimated molecular mass of ∼200 kDa. Peak 2 was 41% of the protein mass and contained particles of 12 ± 6.5 nm radius and an estimated molecular mass of ∼2000 kDa. Although these latter particles contained a significant portion of the mass, they only represent 6% of all particles. Thus, the results of size exclusion chromatography, analytical ultracentrifugation and DLS studies show that Mms6 forms large multimers with most of the particles containing 20−40 protein molecules.

To determine if Mms6 forms micelles, we conducted a series of surface-pressure versus molecular area (π-A) isotherms in a Langmuir trough. We found that the protein distributes spontaneously at the vapor/buffer interface with isotherms that strongly depend on concentration, which is a characteristic of systems that form micelles (Figure 4D). In situ X-ray reflectivity measurements of the films at the vapor/buffer

interface confirmed the formation of a monomolecular Mms6 film at the interface (data not shown).

Being hydrophilic, the C-terminal domain of Mms6 is expected to be located on the surface of a micelle. Therefore, we tested its accessibility to proteolytic cleavage (Figure 4E). Digestion of Mms6 with proteinase K resulted in a significant decrease in its monomeric size within 5 min. This rate of loss of Mms6 molecular mass was similar to the rate of degradation of free C21Mms6 by proteinase K (Figure 4E, bottom panel). A protease-resistant fragment of Mms6 remained after 24 h, whereas BSA was digested almost completely by this time (Figure 4E, top panel). The proteinase K-resistant portion of Mms6 was found as a precipitate, which is consistent with it being part of a hydrophobic resistant core. N-terminal sequencing results confirmed that the precipitate consisted mainly of hydrophobic and aromatic amino acids, as expected from the sequence of the N-terminal domain of Mms6.

Although it has some characteristics of a membrane protein, Mms6 does not require detergent for its solubility in aqueous solution. If it forms a micellar quaternary structure, these micelles might fuse directly with liposomes without the aid of a detergent. To test this question, Mms6 was preincubated at either 4 or 25 °C with liposomes in the presence or absence of Triton X-100 (Figure 4F) and then incubated with a high concentration of proteinase K that completely degrades Mms6 alone, as seen in Figure 4F (last lane). Regardless of the presence of Triton X-100, liposome-preincubated Mms6 was protected from degradation (Figure 4F, lanes 2 and 4). This proteinase K resistant fragment is larger than that produced
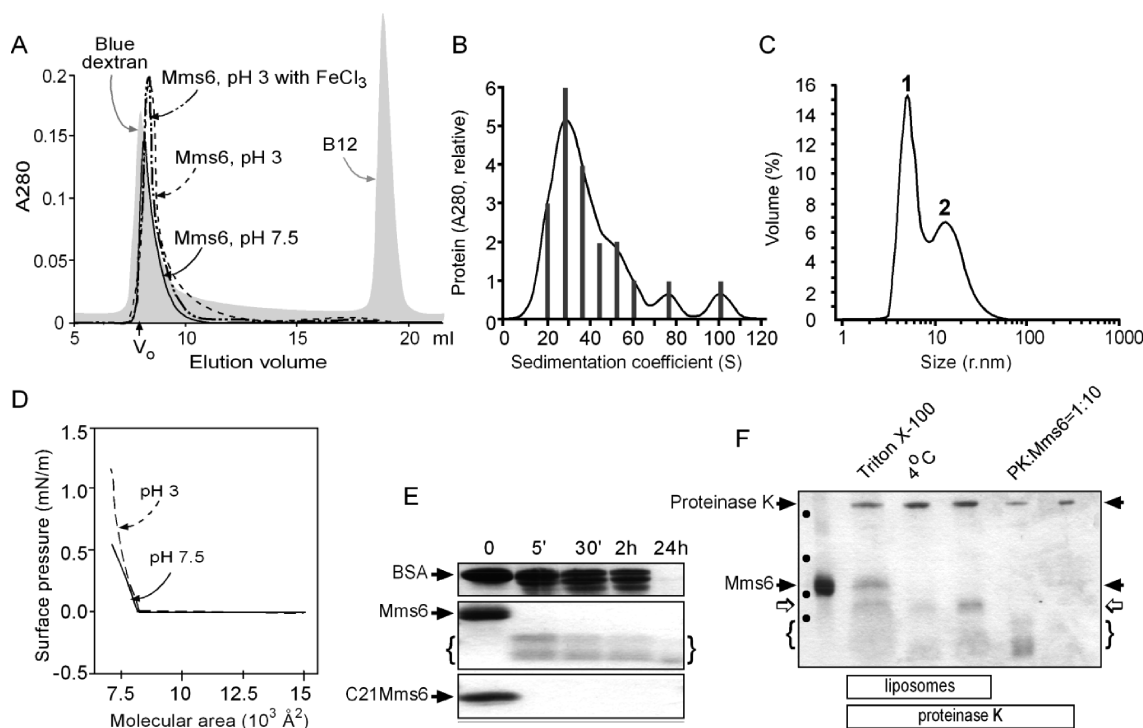
Figure 4. Mms6 self-assembles as micelles. Mms6 assembles into large multimers as shown by the following: (A) Size exclusion chromatography of Mms6 at pH 7.5 (solid line) or pH 3 in the presence or absence of 2 mM $FeCl_3$ (dashed lines). Blue Dextran and vitamin B12 were chromophores included to indicate the positions of the void and salt volumes respectively. (B) The sedimentation velocity profile of Mms6. (C) Dynamic light scattering. (D) Surface pressure vs molecular area isotherms of Mms6 measured in a Langmuir trough on a subphase buffer at pH 7.5 (solid line) or pH 3 (dashed line). (E) Mms6 has a proteinase K resistant core. Mms6 or C21Mms6 (1 mg/mL) was digested by proteinase K [proteinase K/ Mms6 (M/M) = 1:10] for the indicated time periods and then resolved by SDS-PAGE through a 15% acrylamide gel performed as previously described.[34] The curly brackets identify the remaining protease-resistant protein fragments. (F) Mms6/liposome fusion characteristics are consistent with a micellar structure. Mms6 was incubated with and without liposomes and then incubated with proteinase K. Legends above the gel image and the added components listed below the gel image identify the conditions in each tube that deviated from the standard conditions, which were 20 mM Tris, 100 mM KCl, pH 7.5, 25 °C, and proteinase K/Mms6 (M/M) = 1:4. The curly brackets identify the same protease-resistant fragments as in E. The open arrowheads identify the protease-resistant band formed when the protein is associated with liposomes. The dots identify the positions on the gel of the molecular mass markers (from top to bottom: 25, 20, 15, and 10 kDa).

when Mms6 was incubated with proteinase K in the absence of liposomes, which is consistent with the expectation that more of the Mms6 N-terminal domain might be protected from proteolysis when it is buried in the liposome than when in the absence of the liposome, such as in Figure 4E,F, lane 5. Thus, as expected of a micelle, detergent is not required for Mms6 to incorporate into liposomes. The inclusion of Triton X-100 during liposome insertion also resulted in a portion of full-length Mms6 being completely proteinase resistant. This could be due to the trapping of some of the Mms6 either inside the liposomes or occasional inversion of the Mms6 with respect to the liposome membrane resulting in the C-terminus being in the liposome lumen rather than on the outside where it is not accessible to proteinase K. In the absence of liposomes (a control condition), Mms6 was completely degraded at the high proteinase K concentration used in this experiment.

When the temperature during the liposome–protein preincubation period was below the liquid to solid phase transition temperature of the liposomes, Mms6 was less protected from proteinase K digestion (Figure 4F, lane 3). This result is consistent with the hypothesis that Mms6 is incorporated into the liposomes in the absence of detergent by fusion of the protein and lipid micelles, which would be prevented at temperatures below that for the liquid/solid transition.

In summary, we have found that Mms6 (1) forms large relatively homogeneous particles, (2) its C-terminal domain can readily be cleaved, leaving a protease-resistant core, (3) can fuse in a temperature-dependent manner with liposomes, and (4) spreads on an aqueous surface in a Langmuir trough. In their entirety, these results provide strong evidence that Mms6 forms a micellar quaternary structure.

C-Terminal Domain of Mms6 Contributes to Its Quaternary Structure. We examined the role of the C-terminal domain in stabilizing the quaternary structure of Mms6 by determining the effect on micellar stability of mutating the C-terminal domain. The results from size exclusion chromatography showed that, compared with Mms6, m2Mms6 and m3Mms6 formed less stable micelles (Figure 5A). This result suggests that the C-terminal domain itself is involved in forming and maintaining the micellar structure. To examine the multiplicity of C-terminal domain interaction on the micellar surface, we varied the concentration of the C-terminal domain peptide in the presence of a constant concentration of Mms6 (Figure 5B). As the molar ratio of C21Mms6 to Mms6 increased, an increasing amount of the protein precipitated until a ratio of 7:1 (C21Mms6/Mms6) was reached when all of the protein was found as a precipitate. These results suggest that the Mms6 C-terminal domain interacts on the surface of the micelle and that this quaternary structure might be an octamer.
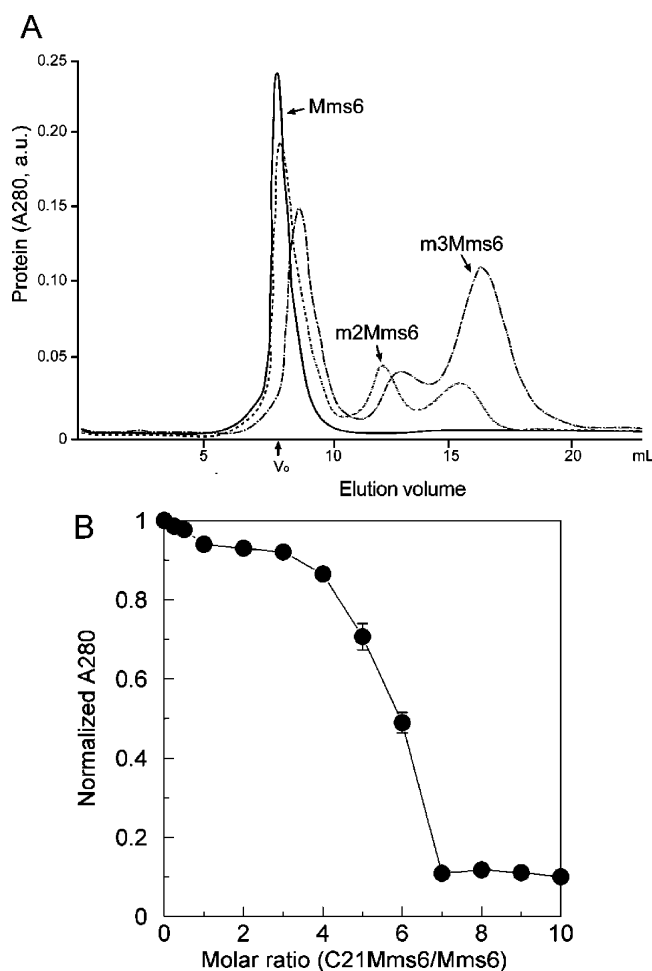
Figure 5. C-Terminal domain contributes to the overall Mms6 quaternary structure. (A) The elution profiles of Mms6, m2Mms6, and m3Mms6 in 20 mM Tris-HCl and 100 mM KCl, pH 7.5, from a Superdex G75 10/300GL column with a flow rate of 0.4 mL/min at 4 °C. All forms of Mms6 include a peak that travels with the void volume. But, for m2Mms6 and m3Mms6, additional peaks are observed that correspond to trimers (~30 kDa) and monomers (~10 kDa) of m2Mms6 and dimers (~20 kDa) and monomers (~10 kDa) of m3Mms6. When examined by denaturing (SDS) PAGE, the samples from all the peaks migrated to the same position, thus, confirming that all peaks on the column contained the same monomeric form of Mms6 mutants. (B) C-Terminal domains of Mms6 interact on the surface of the micelle. A solution of 40 μM Mms6 in 20 mM Tris-HCl and 100 mM KCl, pH 7.5, was titrated with C21Mms6. The absorbance of the supernatant was normalized to 40 μM Mms6. Note that C21 Mms6 has no aromatic amino acids and, therefore, no absorption at 280 nm.

■ DISCUSSION

To understand how a protein, such as Mms6, promotes the nucleation of iron atoms in vitro, yielding crystals of specific size and shape, it is important to know the structure of this protein and how it responds to the presence of iron. With Mms6 being a very small protein (59 amino acids), it seems likely that its relevant functional form involves a larger multimeric assembly. The N-terminal domain of Mms6 contains a Leu-Gly rich region, which is similar to sequences in some self-assembling proteins of other biomineralization systems[26−29] and is consistent with the possibility that Mms6 forms a multimer. Our results show that Mms6 self-assembles

into a uniformly sized micelle of 20−40 units with the C-terminal domain on the surface, and thus, the N-terminal domain is buried, as would be expected from the amphipathic primary sequence of this protein.

Quantitative iron binding studies show that Mms6 binds one Fe^{3+} with a very high affinity ($K_d = 10^{-16}$ M) that we can attribute to the C-terminal domain. This concentration of iron (10^{-16} M) is well below that necessary for magnetite crystal formation, which is in the mM range. To achieve these higher iron concentrations, a lower pH is required. Therefore, we measured Mms6 binding to iron at pH 3, which is the condition used for iron oxide crystal formation promoted by this protein in vitro. Under these conditions, we observed two binding phases with respect to iron concentration; a high affinity phase as discussed and a second low affinity phase (K_d in the μM range). We speculate that both iron-binding phases are likely to be relevant to iron oxide crystal formation. The high affinity stoichiometric binding may contribute to the C-terminal domain adopting an appropriate conformation, whereas the second low affinity iron binding phase in which iron clusters on the protein cooperatively and at high stoichiometry is expected to be involved in crystal building.

The low affinity iron-binding activity of Mms6 is cooperative with respect to iron concentration (Hill n value ~3) and reaches a high stoichiometry of iron/Mms6. The observed cooperativity suggests that the protein organizes the iron on its surface in groups of three iron atoms. This might reflect the beginning of crystal packing as the magnetite crystal structure includes a minimal unit of 2:1 = Fe^{3+}/Fe^{2+}.

We also found that the stoichiometric binding affinity of Mms6 for ferric iron is much higher at pH 7.5 than that at pH 3. Magnetites (Fe_3O_4) are stable in alkaline environments (pH > 7), while hematite (Fe_2O_3) can be stable from pH 1 to pH 14.[30] Studies of *Magnetospirillum magneticum* strain AMB-1 (from which Mms6 is derived) suggest that hematite may be the precursor of magnetite formed by magnetotactic bacteria.[31] We speculate that the pH inside the magnetosome starts low and increases during magnetite formation. The initial stage of magnetite formation is expected to be acidic for ferric iron accumulation and the final stage to be basic for the maturation and stability of magnetites. The in vitro magnetite formation used for this study involves this order of pH change driven by the addition of NaOH to a low pH (HCl) solution containing Mms6. In vivo, the pH of the magnetosome compartment could be regulated by a proton pump. Recent studies from another stain of magnetotactic bacteria, *Magnetospirillum gryphiswaldense*, identified H⁺ transporters that control the formation of magnetites.[32,33]

Mutation of the C-terminal domain of Mms6 by shuffling the −OH and −COOH residues, and leaving the remaining sequence as in the original protein, resulted in the loss of iron binding and a loss of structural integrity. As was Mms6 with a scrambled C-terminal domain, this mutant protein was unable to form superparamagnetic iron oxides and it formed micelles that were less stable than the parent protein. These results suggest that structure of the C-terminal domain is important for stability of the protein micelle. We reasoned that, if the C-terminal domains interact on the surface of the micelles, then additional C-terminal domain peptide might also interact in trans and alter the stability of the micelles. We found that addition of external C-terminal domains resulted in precipitation of Mms6 at a molar ratio of 7:1 peptide/protein. This result shows that the C-terminal domains interact with

each other on the surface of the micelle and suggests that the peptide might form an octamer.

Biomineralization proteins are frequently not large, but are responsible for the formation of large crystal structures. As for many other mineralization proteins, Mms6 self-assembles to form a larger structure that is closer in size to the inorganic assemblages that it promotes.[11−14,19,20] The unusual micellar structure of Mms6 results in a surface of repeated and interacting C-terminal domains and the observed high capacity iron-binding properties of Mms6 may result from the interaction of multiple C-terminal domains that are appropriately spaced for promoting crystal lattice formation. These in vitro observations of Mms6 structure may be relevant to its function both in vitro and in vivo. We speculate that the N-terminal domain is responsible for anchoring the C-terminal domain into the magnetosome membrane in vivo, from which the C-terminal domain interacts with iron to form magnetite nanoparticles. The C-terminal domain may form small protein (octamer) islands as indicated by the in vitro study that initiate crystal seed formation. These small starting seeds might then fuse to produce larger crystal plates as the protein islands move in a fluid hydrophobic environment of the magnetosome membrane. Further investigations are needed to establish the mechanism by which the functional and structural features of Mms6 described here enable this small protein to promote the formation of magnetite nanoparticles of uniform size and shape.

CONCLUSION

In conclusion, we investigated the quaternary structure of Mms6, a biomineralization protein that can promote the formation of magnetite nanoparticles in vitro. We demonstrated that Mms6 forms a unique micellar quaternary structure in vitro that may provide a surface for magnetite crystal formation. Mms6 consists of two subdomains, with the N-terminal domain responsible for anchoring the C-terminal domain in a micelle from which the C-terminal domain interacts with iron to form magnetite nanoparticles. We also quantitatively determined the binding profile of Mms6 with ferric iron and demonstrate that Mms6 has two phases of iron binding, the first is stoichiometric and very high affinity and the second is low affinity, high capacity, and cooperative with respect to iron. We also identified the C-terminal domain of Mms6 to be the functional domain. Taken together, these in vitro studies provide valuable insight toward understanding the mechanism of magnetite nanoparticle formation promoted by Mms6.

ASSOCIATED CONTENT

Ⓢ Supporting Information

Additional experimental details and analytical data. This material is available free of charge via the Internet at http://pubs.acs.org.

AUTHOR INFORMATION

Corresponding Author
*Phone: 515-294-9996. Fax: 515-294-0453. E-mail: marit@iastate.edu.

ACKNOWLEDGMENTS

REFERENCES

(1) Kirschvink, J. L.; Walker, M. M.; Diebel, C. E. *Curr. Opin. Neurobiol.* **2001**, *11*, 462.

(2) Diebel, C. E.; Proksch, R.; Green, C. R.; Neilson, P.; Walker, M. M. *Nature* **2000**, *406*, 299.

(3) Kirschvink, J. L.; Kobayashi-Kirschvink, A.; Woodford, B. J. *Proc. Natl. Acad. Sci. U.S.A.* **1992**, *89*, 7683.

(4) Blakemore, R. *Science* **1975**, *190*, 377.

(5) Balkwill, D. L.; Maratea, D.; Blakemore, R. P. *J. Bacteriol.* **1980**, *141*, 1399.

(6) Ofer, S.; Nowik, I.; Bauminger, E. R.; Papaefthymiou, G. C.; Frankel, R. B.; Blakemore, R. P. *Biophys. J.* **1984**, *46*, 57.

(7) Gorby, Y. A.; Beveridge, T. J.; Blakemore, R. P. *J. Bacteriol.* **1988**, *170*, 834.

(8) Arakaki, A.; Webb, J.; Matsunaga, T. *J. Biol. Chem.* **2003**, *278*, 8745.

(9) Prozorov, T.; Mallapragada, S. M.; Narasimhan, B.; Wang, L.; Palo, P.; Nilsen-Hamilton, M.; Williams, T. J.; Bazylinski, D. A.; Prozorov, R.; Canfield, P. C. *Adv. Funct. Mater.* **2007**, *17*, 951.

(10) Tanaka, M.; Mazuyama, E.; Arakaki, A.; Matsunaga, T. *J. Biol. Chem.* **2011**, *286*, 6386.

(11) Du, C.; Falini, G.; Fermani, S.; Abbott, C.; Moradian-Oldak, J. *Science* **2005**, *307*, 1450.

(12) Weiner, S. *J. Struct. Biol.* **2008**, *163*, 229.

(13) Dey, A.; Bomans, P. H. H.; Müller, F. A.; Will, J.; Frederik, P. M.; With, G. d.; Sommerdijk, N. A. J. M. *Nat. Mater.* **2010**, *9*, 1010.

(14) Cölfen, H. *Nat. Mater.* **2010**, *9*, 960.

(15) Simons, K.; Helenius, A.; Leonard, K.; Sarvas, M.; Gething, M. J. *Proc. Natl. Acad. Sci. U.S.A.* **1978**, *75*, 5306.

(16) Liu, D.; Tian, H.; Kumar, R.; Zhang, L. *Macromol. Rapid Commun.* **2009**, *30*, 1498.

(17) Lakshminarayanan, R.; Vivekanandan, S.; Samy, R. P.; Banerjee, Y.; Chi-Jin, E. O.; Teo, K. W.; Jois, S. D.; Kini, R. M.; Valiyaveettil, S. *J. Am. Chem. Soc.* **2008**, *130*, 4660.

(18) Moradian-Oldak, J.; Paine, M. L.; Lei, Y. P.; Fincham, A. G.; Snead, M. L. *J. Struct. Biol.* **2000**, *131*, 27.

(19) Fincham, A. G.; Moradian-Oldak, J.; Diekwisch, T. G.; Lyaruu, D. M.; Wright, J. T.; Bringas, P. Jr.; Slavkin, H. C. *J. Struct. Biol.* **1995**, *115*, 50.

(20) Fincham, A. G.; Moradian-Oldak, J.; Simmer, J. P.; Sarte, P.; Lau, E. C.; Diekwisch, T.; Slavkin, H. C. *J. Struct. Biol.* **1994**, *112*, 103.

(21) Van Holde, K. E.; Weischet, W. O. *Biopolymers* **1978**, *17*, 1387.

(22) Demeler, B.; van Holde, K. E. *Anal. Biochem.* **2004**, *335*, 279.

(23) Demeler, B. The University of Texas Health Science Center at San Antonio, Department of Biochemistry. http://www.ultrascan.uthscsa.edu.

(24) Lu, X.; Zhang, Y.; Shin, Y.-K. *Nat. Struct. Mol. Biol.* **2008**, *15*, 700.

(25) Prozorov, T.; Palo, P.; Wang, L.; Nilsen-Hamilton, M.; Jones, D.; Orr, D.; Mallapragada, S. K.; Narasimhan, B.; Canfield, P. C.; Prozorov, R. *ACS Nano* **2007**, *1*, 228.

(26) Amemiya, Y.; Arakaki, A.; Staniland, S. S.; Tanaka, T.; Matsunaga, T. *Biomaterials* **2007**, *28*, 5381.

(27) Schüler, D. *FEMS Microbiol. Rev.* **2008**, *32*, 654.

(28) Faivre, D.; Schüler, D. *Chem. Rev.* **2008**, *108*, 4875.

(29) Komeili, A. *Annu. Rev. Biochem.* **2007**, *76*, 351.

(30) Bell, P. E.; Mills, A. L.; Herman, J. S. *Appl. Environ. Microbiol.* **1987**, *53*, 2610.

(31) Staniland, S.; Ward, B.; Harrison, A.; van der Laan, G.; Telling, N. *Proc. Natl. Acad. Sci. U.S.A.* **2007**, *104*, 19524.

(32) Uebe, R.; Junge, K.; Henn, V.; Poxleitner, G.; Katzmann, E.; Plitzko, J. M.; Zarivach, R.; Kasama, T.; Wanner, G.; Pósfai, M.; Böttger, L.; Matzanke, B.; Schüler, D. *Mol. Microbiol.* **2011**, In press.

(33) Nies, D. H. *Mol. Microbiol.* **2011**, In press.

(34) Thalacker, F. W.; Nilsen-Hamilton, M. *J. Biol. Chem.* **1987**, *262*, 2283.